



Tracing transport of chitosan nanoparticles and molecules in Caco-2 cells by fluorescent labeling

Xiaoyan Jia^a, Xue Chen^b, Yinglei Xu^a, Xinyan Han^a, Zirong Xu^{a,*}

^aNano-biology Lab of Animal Science College, Zhejiang University, Qiantao North Road 164, Hangzhou 310029, China

^bAgriculture College, Yanbian University, Longjing 133400, Jilin, China

ARTICLE INFO

Article history:

Received 11 February 2009

Received in revised form 9 April 2009

Accepted 16 April 2009

Available online 3 May 2009

Keywords:

Chitosan nanoparticles

Chitosan

Fluorescent labeling

Caco-2

Cytotoxicity

Transport

ABSTRACT

The aim of this study was to explore the transport properties of chitosan nanoparticles and molecules in Caco-2 cells. Fluorescein isothiocyanate-labeled chitosan (f-CS) was synthesized and prepared into nanoparticles (f-CNP). The f-CNP exhibit a mean size of 58.04 nm and a mean charge with +41.63 mV. Cytotoxicities of the f-CNP and the f-CS against Caco-2 cells were disregarded in the transport study. The transport was observed under fluorescence microscope. The f-CNP could be transported into Caco-2 cells across the cell membrane, and showed concentration-dependent and saturable intracellular fluorescence signal at 37 °C. Meanwhile, the energy-dependence of the trans-membrane transport of f-CNP was not observed at 4 °C. The f-CS was mainly accumulated in the cell peripheral and showed a concentration-dependent intercellular fluorescence signal. Thus, formulation of chitosan into nanoparticles significantly improved its trans-membrane transport in Caco-2 cells.

Crown Copyright © 2009 Published by Elsevier Ltd. All rights reserved.

1. Introduction

Chitosan is the partially deacetylated product of chitin which is the primary component of exoskeletons of crustaceans and insects as well as of cell walls of some fungi. Chitosan exhibits a variety of physicochemical and biological properties resulting in applications in numerous fields such as waste water treatment, agriculture, textiles, dyeing and food processing (Kumar, 2000). In addition to its low toxicity, biocompatibility and biodegradability, chitosan have attracted attention for application in pharmaceutical and medical fields (Illum, 1998). The co-administration of chitosan and its derivatives leads to a strongly improved bioavailability of many perorally given drugs such as busserelin, calcitonin and insulin (Ma, Lim, & Lim, 2005; Takeuchi, Matsui, Yamamoto, & Kawashima, 2003; Thanou, Florea, Langemeyer, Verhoef, & Junginger, 2000).

Chitosan-based particulate systems, especially chitosan nanoparticles, have been exploited as carriers for oral delivery of peptides, proteins, and nucleotides (Luessen et al., 1996; Pan et al., 2002; Roy, Mao, Huang, & Leong, 1999). Besides this, it also has bioactive properties in its own right. Previous studies from our lab have demonstrated that chitosan nanoparticles per se exhibit superior anticancer activity both *in vitro* and *in vivo* by oral administration (Qi & Xu, 2006; Qi, Xu, & Chen, 2007; Qi, Xu, Jiang, Li, & Wang, 2005). In these researches, it is of high importance to assess the uptake effectiveness of chitosan nanoparticles into their target site. Therefore, it is imperative to eval-

uate the absorption of chitosan nanoparticles in the human intestine. It could be of significant importance in improving chitosan nanoparticles bioavailability and optimizing chitosan nanoparticles-based oral drug delivery systems.

The objectives of the present study were to characterize the transport of chitosan nanoparticles and molecules in human intestinal epithelium. The transport study was performed using fluorescein-labeled chitosan nanoparticles (f-CNP) and molecules (f-CS) on confluent human colon carcinoma (Caco-2) cell monolayers to visually display the transport under different conditions.

2. Materials and methods

2.1. Materials

The chitosan used in this study was obtained from the Zhejiang Golden-Shell Biochemical Co., Ltd. (Zhejiang, China). The deacetylation degree was about 86% as determined by elemental analysis, and the average molecular weight of the chitosan was around 200 kDa as determined by viscometric methods.

The human colon carcinoma cell line (Caco-2) was obtained from Shanghai Institute of Cell Biology, Chinese Academy of Science.

High glucose Dulbecco's modified Eagle medium (DMEM, containing 4.5 g/L glucose), heat-inactivated fetal bovine serum (FBS), penicillin–streptomycin solution, trypsin–EDTA, L-glutamine, nonessential amino acids and Hank's Balanced Salt Solution (HBSS) were purchased from Gibco-BRL Life Technology

* Corresponding author. Tel.: +86 571 86971075; fax: +86 571 86994963.
E-mail address: zrxu@zju.edu.cn (Z. Xu).

(Grand Island, NY, USA). Fluorescein isothiocyanate (FITC), 3-(4,5-dimethylthiazol-2-yl)-2,5-diphenyl-tetrazolium bromide (MTT), tripolyphosphate sodium (TPP) and trypan blue were purchased from Sigma Chemical Co. (St. Louis, MO, USA). The ultrapure deionized water used throughout this study was prepared with a Milli-Q SP reagent water system (Millipore, Milford, MA, USA). All other chemicals were of analytical grade commercially obtained from local chemical suppliers.

2.2. Preparation of the f-CS

The preparation of f-CS was according to a previously reported procedure (Huang, Ma, Khor, & Lim, 2002). One-gram chitosan was dissolved in 100 mL of 0.1 M acetic acid, added 100 mL dehydrate methanol to it and stirred. About 50 mL FITC (2.0 mg/mL) in methanol was slowly added to the chitosan solution. The reaction was pre-ceeded for 4 h at room temperature in the dark, and then precipitated the labeled polymer in 0.5 M NaOH by arising pH to 8–9. The precipitate was centrifuged (40,000g, 10 min) and washed by acetone: water (3:1 v/v) repeatedly until no fluorescence was detected in the supernatant (Perkin Elmer Inc., luminescence spectrometer LS50B, λ_{exc} 485 nm, λ_{emi} 520 nm). Followed, the f-CS was dissolved in 0.1 M acetic acid and dialyzed in water for 3 days in the dark before freeze drying (Vitrisc Co. Inc., Gardiner, New York). To determine the labeling efficiency, a specified amount of the f-CS dissolved in 0.1 M acetic acid and the fluorescence intensity was measured. The fluorometer was calibrated with standard solutions of 0.001–0.09 $\mu\text{g}/\text{mL}$ of FITC in the same solution. Labeling efficiency (percent) was calculated as the percent weight of FITC to weight of the f-CS.

2.3. Preparation and characterization of the f-CNP

The f-CS was transformed into the f-CNP by ionic gelation with negatively charged TPP ions according to a previously reported procedure (Ma & Lim, 2003). Nanoparticles spontaneous formed by slowly adding 4 mL of 0.10% TPP in water to 8 mL of 0.25% f-CS in 0.1 M acetic acid with stirring at 1000 rpm at ambient temperature. Zeta potential and particle size of the nanoparticles were characterized immediately upon preparation using Zetasizer Nano-ZS90 (Malvern Instruments Ltd., UK). The samples were diluted with distilled water and measured at 25 °C with a scattering angle of 90°. Atomic force microscopy (AFM, SPM-9500J3) was used for visualization the morphology of the f-CNP deposited on mica substrates operating in the contact mode.

In vitro release of FITC was evaluated by high-speed centrifugation (70,000g, 30 min) of the f-CNP and the f-CS after incubated with the complete cell culture medium (90% DMEM + 10% FBS) used in the following transport study for 2 h, the fluorescence intensity of the supernatants were determined by a fluorometer (λ_{exc} 485 nm, λ_{emi} 520 nm).

2.4. Caco-2 cell culture

The Caco-2 cells were normally cultured and maintained in high glucose (4.5 mg/L) DMEM, supplemented with 10% (v/v) FBS, 2 mM L-glutamine, 1%(v/v) nonessential amino acids, 100 U/mL penicillin G and 100 $\mu\text{g}/\text{mL}$ streptomycin. Expand and cultivate cells in a cell culture incubator set at 37 °C, 5% CO₂ and 95% relative humidity. Caco-2 cell monolayers usually reach confluence after 5 ± 1 days. After reaching 80% confluence, cells were digested by using 0.25% trypsin containing 1 mM EDTA. Cells of passage numbers 30–40 were used throughout.

2.5. Cytotoxicity evaluation

The determination of cell viability is a common assay to evaluate the *in vitro* cytotoxicity of biomaterials. The cytotoxicities of the f-CNP and the f-CS against Caco-2 cells were determined by MTT assay. The cells were seeded onto 96 well plate at a density of 1×10^4 cell/well in 100 μL medium for 24 h in the CO₂ incubator. The medium in each well were replaced with the f-CNP or the f-CS and diluted with culture medium to give a chitosan concentration of 50–1000 $\mu\text{g}/\text{mL}$ (pH 7.4). After 4 h incubation at 37 °C, the f-CNP and the f-CS were replaced with 100 μL MTT (0.5 mg/mL in HBSS, pH 7.4) and incubated for another 4 h at 37 °C. Subsequently, the MTT medium was pipette off from the wells and the formazan crystals were dissolved in DMSO, gentle shaking for 10 min to achieve complete dissolution. The absorbance of the resultant solutions was measured at 490 nm using a Bio-Rad microplate reader. The control wells received complete culture medium with cells. Each concentration of the samples had six replicates. Every test includes a blank containing complete medium without cells. The viability was presented as the percent of sample well to the control well.

2.6. Transport study

Caco-2 cells were seeded on 12-well plate at a density of 5×10^4 cells/cm² and used for transport studies on days 6 and 7 on confluency. The freshly prepared f-CNP and f-CS was diluted with HBSS (pH 7.4) to give equivalent chitosan concentrations of 50–1000 $\mu\text{g}/\text{mL}$. The transport studies were initiated by rinsing each cell monolayer with HBSS three times. The diluted chitosan samples were added to each well (1 mL) for incubation with Caco-2 cells. The transport experiments were terminated by washing the cell monolayers thrice with ice-cold HBSS. For quenching the fluorescence of FITC-labeled compounds on the cell surface, the cell monolayers were mildly washed twice with trypan blue solution (100 $\mu\text{g}/\text{mL}$), and then the Caco-2 cells were observed and photographed by fluorescence microscope (Olympus IX-71, Japan).

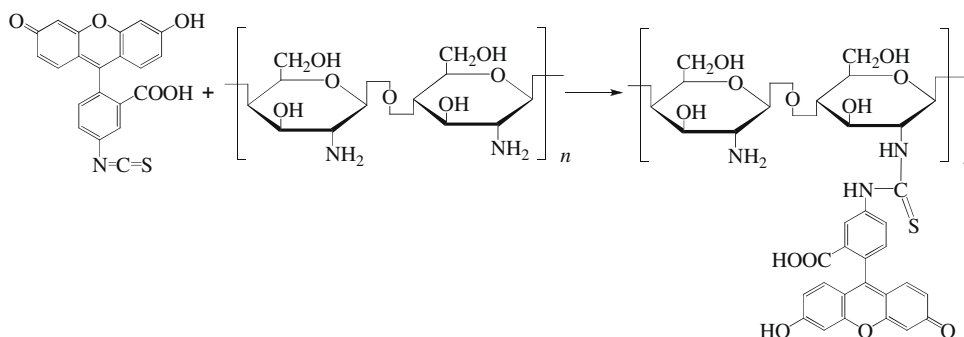


Fig. 1. Schematic diagram of the reaction between FITC and chitosan.

3. Results and discussion

3.1. Labeling reaction

The labeling reaction was based on the covalent binding between the isothiocyanate group of FITC and the primary amino group of D-glucosamine as shown in Fig. 1. The reaction yielded a fluorescent yellow polymer and the weight fraction of FITC per unit weight of chitosan was 1.78% (w/w).

As regards to the stability of the labeled polymer, *in vitro* release study was carried out. The results showed that no released FITC was detected from the f-CS and f-CNP after incubation with the DMEM for 2 h *in vitro*. Accordingly, the fluorescent labeling in this study provided a stable fluorescent signal without interference of the dissociative FITC.

3.2. Characterization of f-CNP

Particle size and zeta potential are important characteristics of nanoparticles. The results in Fig. 2 showed that the resulting nanoparticles had small sizes and positive surface potentials. The size of the f-CNP ranges from 51.68 to 73.21 nm, and the mean size were

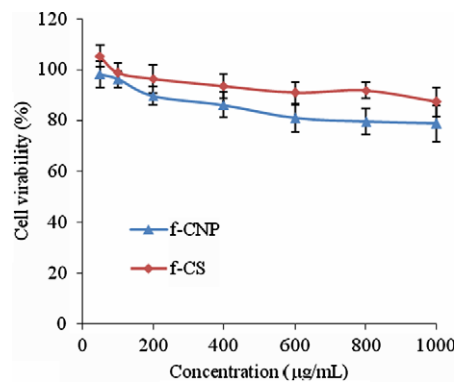


Fig. 3. *In vitro* cytotoxicities of the f-CNP and the f-CS on Caco-2 cells as measured by the MTT assay. Values represent means \pm SD ($n = 6$).

about 58.04 nm. The zeta potential represents the charge of the particle surface. As the zeta potential increases, the repulsive interactions will be larger leading to the formation of more stable particles with a more uniform size distribution. In a sense, the zeta

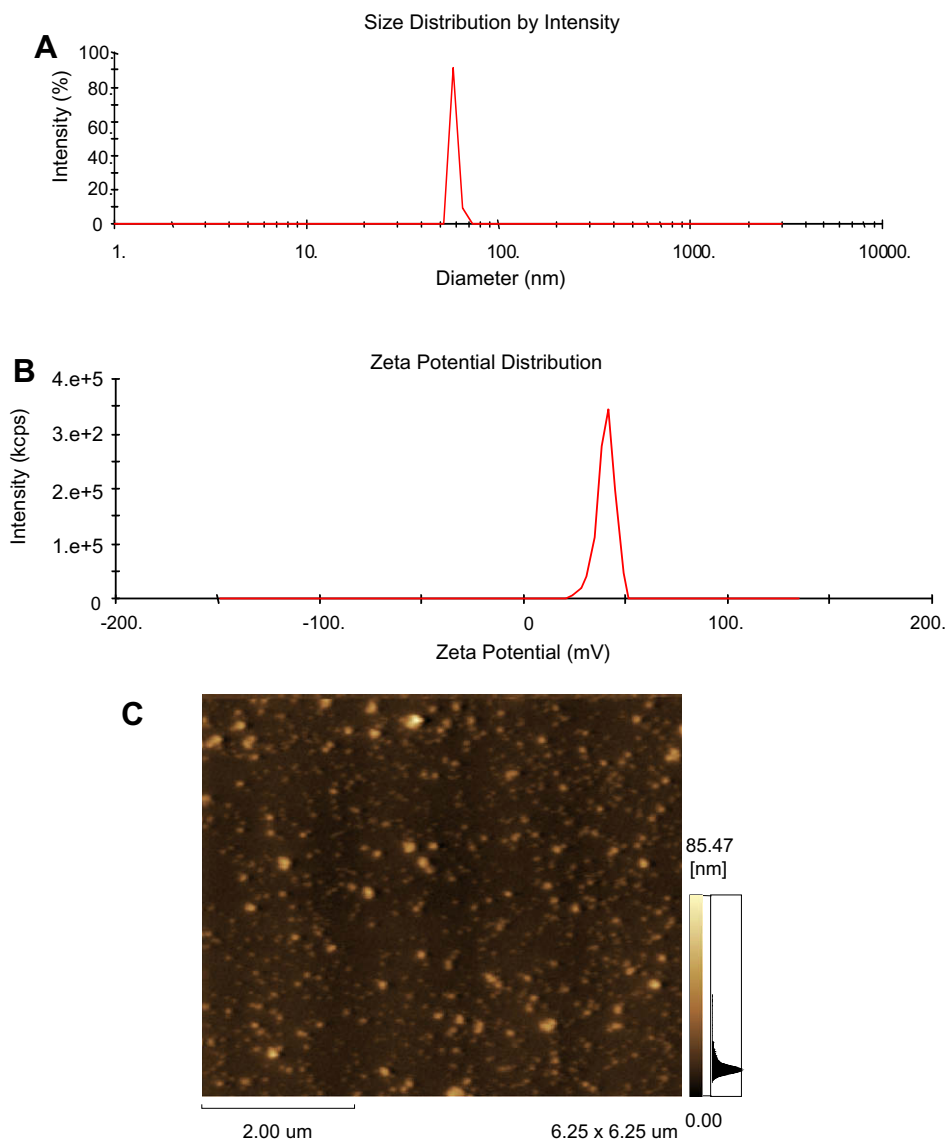


Fig. 2. (A) Size distribution of the f-CNP. The size of f-CNP ranges from 51.68 to 73.21 nm, and the mean size are about 58.04 nm. (B) The zeta potential distribution of the f-CNP. They exhibit a zeta potential range from 40.19 to 44.48 mV and have a mean charge with 41.63 mV. (C) Atomic force micrograph (AFM) of the f-CNP.

potential reflects a parameter for particle stability. A physically stable nanosuspension solely stabilized by electrostatic repulsion will have a minimum zeta potential of ± 30 mV (Muller, Jacobs, & Kayser, 2001). This stability is important in preventing aggregation. The f-CNP prepared in this study showed the zeta potential ranges from +40.19 to +44.48 mV and has a mean charge with +41.63 mV. The Atomic Force Micrographs also proved that the f-CNP have a fine dispersion and conformance of particle size. Although paired *t* test ($p < 0.05$) suggested that the FITC-conjugation significantly changed the particle size and the zeta potential compared with the parent chitosan nanoparticles (Qi, Xu, Jiang, Hu, & Zou, 2004), it should be noted that there were considerable overlaps in their zeta potential ranges.

3.3. Cytotoxicity evaluation

The cell viability of Caco-2 cells after incubated with the f-CNP and the f-CS for 4 h was shown in Fig. 3. Neither the f-CNP nor the f-CS at 50 $\mu\text{g}/\text{mL}$ showed toxicity against the Caco-2 cells, which were compared with control. Both of them showed toxicity to the metabolism of the Caco-2 cells at higher concentration. They produced dose-dependent inhibitory effects but not linear. The cell viability was lower by incubation with the f-CNP than the f-CS at the same concentration. The difference in cytotoxicity mainly lies in the molecular weight as well as the cationic charge density, which were confirmed as key parameters of chitosan for the interaction with the cell membranes and consequently, the cell damage

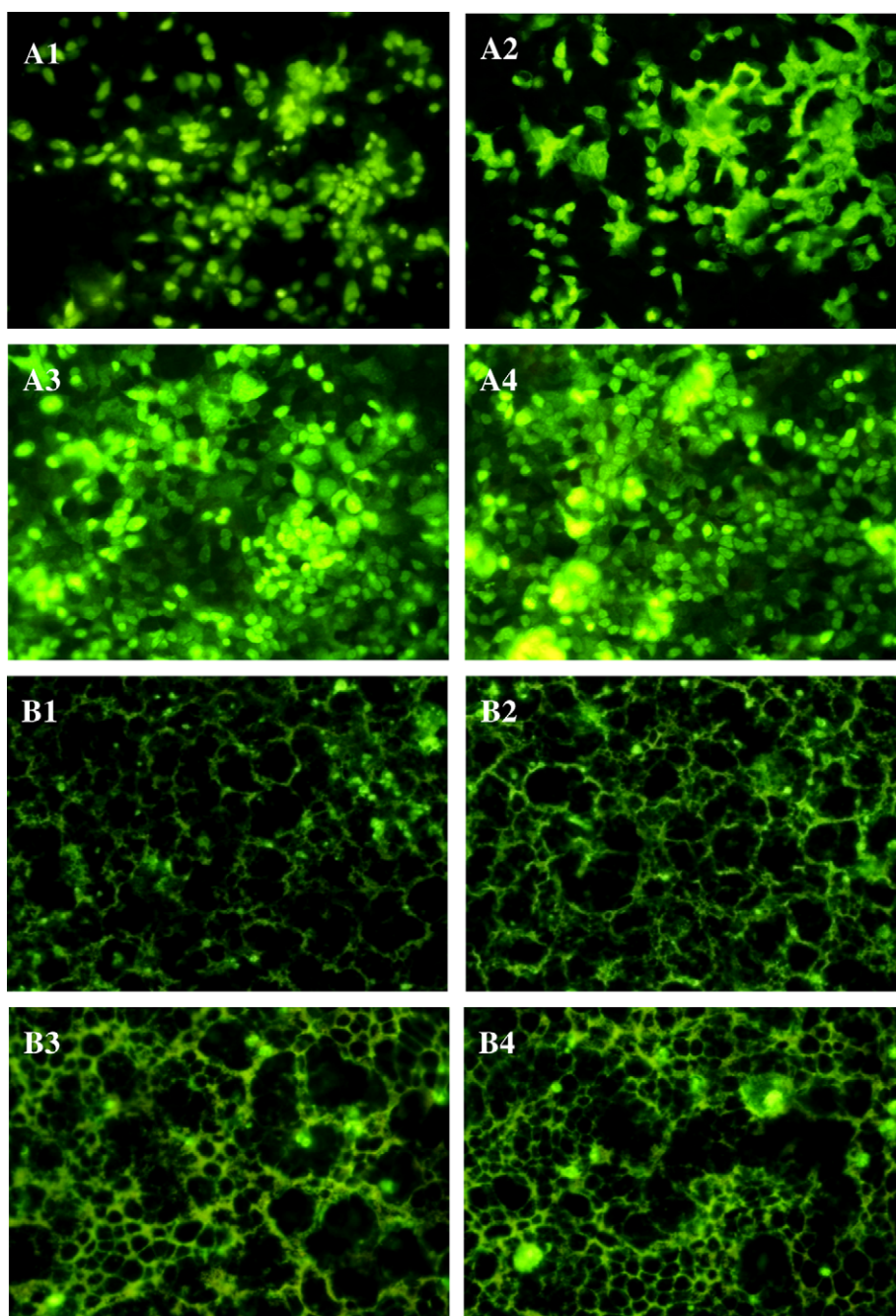


Fig. 4. Fluorescence images of Caco-2 cell monolayers incubated with the f-CNP and the f-CS at various concentrations for 2 h at 37 °C. A1–A4 represents incubation with the f-CNP at 50, 100, 250 and 500 $\mu\text{g}/\text{mL}$, respectively; B1–B4 represents incubation with the f-CS at 50, 100, 250 and 500 $\mu\text{g}/\text{mL}$, respectively.

(Fischer, Li, Ahlemeyer, Krieglstein, & Kissel, 2003). Some researchers had pointed out that the cellular uptake of chitosan and chitosan nanoparticles was not associated with their cytotoxicity (Huang, Khor, & Lim, 2004). In this study, Caco-2 cell detachment and suspension was not observed by incubation with the f-CNP and the f-CS under 600 $\mu\text{g}/\text{mL}$ for 4 h. Therefore, the effect of the cytotoxicity of the fluorescence-labeled chitosan samples on Caco-2 cells was disregarded in the following transport studies.

3.4. Effects of concentration on the transport

Sample concentration was an important factor in transport. Fig. 4 shows the effects of concentration on the transport of the f-CNP and the f-CS at 37 $^{\circ}\text{C}$. The intracellular fluorescence signals after incubation with the f-CNP showed that the f-CNP could be

transported across the Caco-2 cell membrane into the cell interior. According to the fluorescence intensity, the uptake of the f-CNP was concentration-dependent at the range of 50–250 $\mu\text{g}/\text{mL}$, and no great difference between 250 $\mu\text{g}/\text{mL}$ and 500 $\mu\text{g}/\text{mL}$ or even higher concentrations (images not presented). So, it can be deduced that the trans-membrane transport of the f-CNP was a saturation process.

In contrast, the cell associated f-CS was mainly located in the intercellular space and showed extracellular fluorescence signals (Fig. 4B1–B4). The higher the concentration, the stronger the extracellular fluorescence signals. The f-CS showed a concentration-dependent and unsaturated process in the concentration range studied.

It was known that chitosan and cell membranes were interacted by nonspecific electrostatic forces of attraction (Schipper et al.,

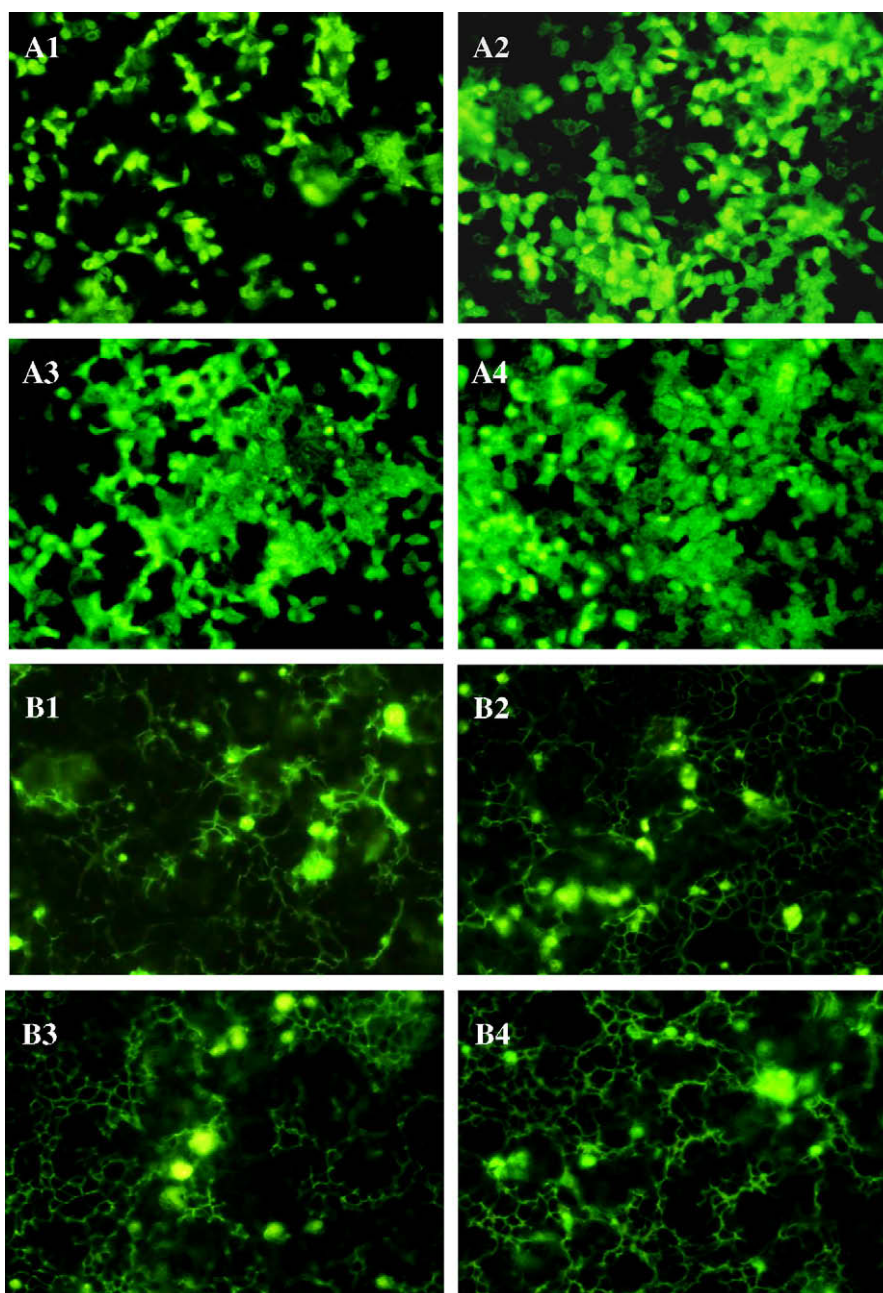


Fig. 5. Fluorescence images of Caco-2 cell monolayers co-incubated with the f-CNP and the f-CS for different time at 37 $^{\circ}\text{C}$. A1–A4 represents incubation with the f-CNP (250 $\mu\text{g}/\text{mL}$) for 30, 60, 90 and 120 min, respectively; B1–B4 represents incubation with the f-CS (250 $\mu\text{g}/\text{mL}$) for 30, 60, 90 and 120 min, respectively. All pictures were magnified by 200-fold.

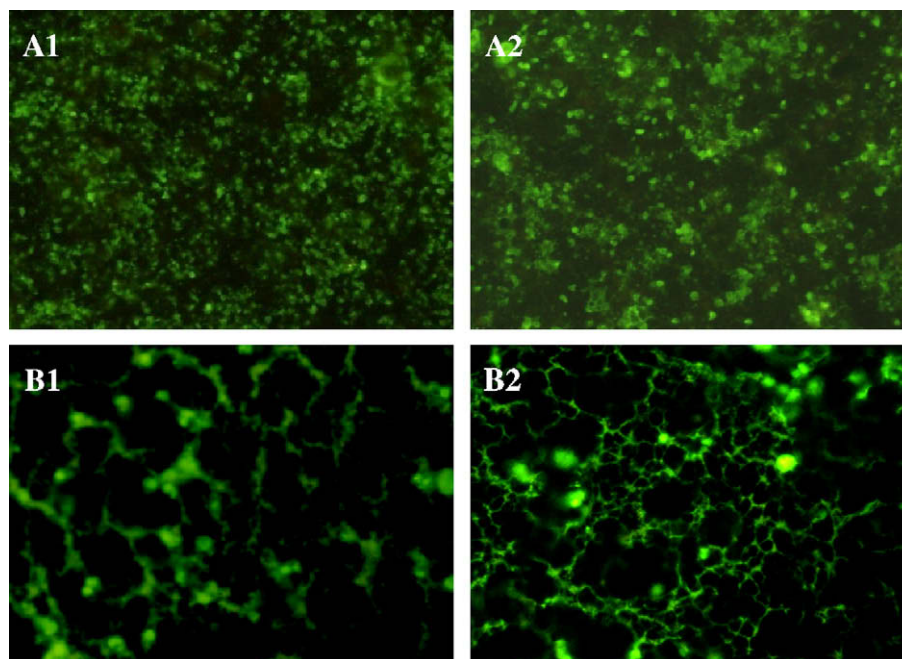


Fig. 6. Fluorescence images of Caco-2 cell monolayers co-incubated with f-CNP and f-CS at different temperature for 2 h. A1, A2 (50-fold magnified) represent incubation with the f-CNP (250 $\mu\text{g}/\text{mL}$) at 4 $^{\circ}\text{C}$ and 37 $^{\circ}\text{C}$, respectively; B1, B2 (200-fold magnified) represent incubation with the f-CS (250 $\mu\text{g}/\text{mL}$) at 4 $^{\circ}\text{C}$ and 37 $^{\circ}\text{C}$, respectively.

1997). Therefore, the transport was initiated by nonspecific electrostatic force. The positive charged f-CNP exhibits a strong attraction to the negatively charged cell membrane (Yamasaki et al., 2002). However, the f-CS was not transported into Caco-2 cells after adhesion. That is the reason for the amount of the f-CNP transported into Caco-2 cells greatly higher than that of the f-CS at all the tested concentrations for 2 h at 37 $^{\circ}\text{C}$.

3.5. Effects of time on the transport

With respect to the time effects on the transport, the results in Fig. 5 showed both of the f-CNP and the f-CS transport were time-dependent processes in 2 h. The uptake of the f-CNP was rapid with fluorescence microscopy demonstrating their localization mostly in the cytoplasm for 30 min incubation (Fig. 5A1). With time progressing, the uptake amounts of the f-CNP were increased. Cellular transport of the f-CS, which should vividly expressed as cellular adhesion in this study, was also linear with time for up to 2 h (Fig. 5B1–B4).

3.6. Effects of temperature on the transport

Effects of temperature on the transport were shown in Fig. 6. The uptake of the f-CNP (250 $\mu\text{g}/\text{mL}$) by Caco-2 cells at 4 $^{\circ}\text{C}$ (Fig. 6A1) and 37 $^{\circ}\text{C}$ (Fig. 6A2) had no distinctive difference. This meant that the transport of the f-CNP was not energy-dependent. The intracellular fluorescence signals of the f-CS at 4 $^{\circ}\text{C}$ (Fig. 6B1) showed the changed fluidity of cell membrane by temperature could facilitate the transport of f-CNP into Caco-2 cells.

Many membrane transport studies on carbohydrates have shown that three mechanisms, active transport, facilitated transport, and passive diffusion/paracellular transport (Tsuji & Tamai, 1996), operate in parallel for the transfer of these hexoses into blood stream. Because the transport of the f-CNP by the Caco-2 cells was a saturable process, the nanoparticles were unlikely to be transported by passive diffusion. Carrier-mediated transport is energy-dependent, and no receptor specific to chitosan has been reported to exist in cell membranes. Therefore, active transport

was unlikely to participate in the transport of the f-CNP by Caco-2 cells.

4. Conclusion

The present study can be considered as innovative to improve our understanding of the process of absorption of chitosan nanoparticles in the human intestinal epithelium. Formulation of chitosan into nanoparticles significantly improved its trans-cellular transport in Caco-2 cells. As the fluorescent-labeled nanoparticles can provide a rapid, simple, and sensitive means to determine cell-associated nanoparticles by fluorometry (Delie, 1998), a quantitative evaluation of the transport of chitosan nanoparticles and molecules in intestinal cells should be further studied based on this study to clarify the transport mechanism of them.

Acknowledgements

The financial support of the Zhejiang Science and Technology Council (No. 2008C22037) is gratefully acknowledged.

References

- Fischer, D., Li, Y. X., Ahlemeyer, B., Krieglstein, J., & Kissel, T. (2003). In vitro cytotoxicity testing of polycations: Influence of polymer structure on cell viability and hemolysis. *Biomaterials*, 24(7), 1121–1131.
- Huang, M., Khor, E., & Lim, L. Y. (2004). Uptake and cytotoxicity of chitosan molecules and nanoparticles: Effects of molecular weight and degree of deacetylation. *Pharmaceutical Research*, 21(2), 344–353.
- Huang, M., Ma, Z., Khor, E., & Lim, L. Y. (2002). Uptake of FITC-chitosan nanoparticles by A549 cells. *Pharmaceutical Research*, 19(10), 1488–1494.
- Illum, L. (1998). Chitosan and its use as a pharmaceutical excipient. *Pharmaceutical Research*, 15(9), 1326–1331.
- Kumar, M. N. V. R. (2000). A review of chitin and chitosan applications. *Reactive & Functional Polymers*, 46(1), 1–27.
- Luessen, H. L., de Leeuw, B. J., Langemeyer, M. W., de Boer, A. B., Verhoef, J. C., & Junginger, H. E. (1996). Mucoadhesive polymers in peroral peptide drug delivery. VI. Carbomer and chitosan improve the intestinal absorption of the peptide drug buserelin in vivo. *Pharmaceutical Research*, 13(11), 1668–1672.

- Ma, Z., & Lim, L. Y. (2003). Uptake of chitosan and associated insulin in Caco-2 cell monolayers: A comparison between chitosan molecules and chitosan nanoparticles. *Pharmaceutical Research*, 20(11), 1812–1819.
- Ma, Z., Lim, T. M., & Lim, L. Y. (2005). Pharmacological activity of peroral chitosan–insulin nanoparticles in diabetic rats. *International Journal of Pharmaceutics*, 293(1–2), 271–280.
- Muller, R. H., Jacobs, C., & Kayser, O. (2001). Nanosuspensions as particulate drug formulations in therapy Rationale for development and what we can expect for the future. *Advanced Drug Delivery Reviews*, 47(1), 3–19.
- Pan, Y., Li, Y. J., Zhao, H. Y., Zheng, J. M., Xu, H., Wei, G., et al. (2002). Bioadhesive polysaccharide in protein delivery system: Chitosan nanoparticles improve the intestinal absorption of insulin in vivo. *International Journal of Pharmaceutics*, 249(1–2), 139–147.
- Qi, L., Xu, Z., & Chen, M. (2007). In vitro and in vivo suppression of hepatocellular carcinoma growth by chitosan nanoparticles. *European Journal of Cancer*, 43(1), 184–193.
- Qi, L. F., & Xu, Z. R. (2006). In vivo antitumor activity of chitosan nanoparticles. *Bioorganic & Medicinal Chemistry Letters*, 16(16), 4243–4245.
- Qi, L. F., Xu, Z. R., Jiang, X., Hu, C. H., & Zou, X. F. (2004). Preparation and antibacterial activity of chitosan nanoparticles. *Carbohydrate Research*, 339(16), 2693–2700.
- Qi, L. F., Xu, Z. R., Jiang, X., Li, Y., & Wang, M. Q. (2005). Cytotoxic activities of chitosan nanoparticles and copper-loaded nanoparticles. *Bioorganic & Medicinal Chemistry Letters*, 15(5), 1397–1399.
- Roy, K., Mao, H. Q., Huang, S. K., & Leong, K. W. (1999). Oral gene delivery with chitosan–DNA nanoparticles generates immunologic protection in a murine model of peanut allergy. *Nature Medicine*, 5(4), 387–391.
- Schipper, N. G. M., Olsson, S., Hoogstraate, J. A., deBoer, A. G., Varum, K. M., & Artursson, P. (1997). Chitosans as absorption enhancers for poorly absorbable drugs. 2. Mechanism of absorption enhancement. *Pharmaceutical Research*, 14(7), 923–929.
- Takeuchi, H., Matsui, Y., Yamamoto, H., & Kawashima, Y. (2003). Mucoadhesive properties of carbopol or chitosan-coated liposomes and their effectiveness in the oral administration of calcitonin to rats. *Journal of Controlled Release*, 86(2–3), 235–242.
- Thanou, M., Florea, B. I., Langemeyer, M. W. E., Verhoef, J. C., & Junginger, H. E. (2000). N-trimethylated chitosan chloride (TMC) improves the intestinal permeation of the peptide drug buserelin in vitro (Caco-2 cells) and in vivo (rats). *Pharmaceutical Research*, 17(1), 27–31.
- Tsuji, A., & Tamai, I. (1996). Carrier-mediated intestinal transport of drugs. *Pharmaceutical Research*, 13(7), 963–977.
- Yamasaki, Y., Sumimoto, K., Nishikawa, M., Yamashita, F., Yamaoka, K., Hashida, M., et al. (2002). Pharmacokinetic analysis of in vivo disposition of succinylated proteins targeted to liver nonparenchymal cells via scavenger receptors: Importance of molecular size and negative charge density for in vivo recognition by receptors. *Journal of Pharmacology and Experimental Therapeutics*, 301(2), 467–477.